Mean-field theory of multilayer physisorption. III. Desorption kinetics

E. Sommer* and H. J. Kreuzer
Theoretical Physics Institute, Department of Physics, University of Alberta, Edmonton, Alberta T6G 2J1, Canada
(Received 1 June 1982)

Starting from a set of nonlinear rate equations with phonon-mediated transition probabilities calculated from the self-consistent solutions of temperature-dependent mean-field theory, we calculate temperature- and coverage-dependent desorption times for the ^{3}He-graphite, ^{4}He-graphite, ^{3}He-Ar(100), and ^{3}He-Constantan systems up to a coverage of two monolayers. We find (a) a significant drop in the heat of adsorption and in the prefactor, (b) a pronounced compensation effect, and (c) a change over from first-order desorption at low coverage to zero-order evaporation for $\Theta > 1.5$.

I. INTRODUCTION

Studies of adsorption and desorption kinetics of a gas in front of the surface of a solid are made in an attempt to elucidate the mechanisms by which gas particles dissipate or acquire energy to overcome the attractive forces that bind them to the surface. Whereas for chemisorbed gases electronic degrees of freedom are mediating the adsorption and desorption processes, the latter are predominantly realized by the lattice vibrations of the solid for physisorbed gases. We recall that a gas particle is said to physisorb onto the surface of a solid if the net interaction between a gas particle and the solid is accounted for by an effective wall or surface potential $V_s(\vec{r})$, the long-range part of which is essentially the interaction energy between the mutually induced fluctuating dipole moments on the adsorbing gas particle and in the solid. The strong short-range repulsion is largely due to increasing charge fluctuations as the adsorbing particle becomes confined close to the surface. For an inert gas atom at position $\vec{r}$ in front of a molecular solid, $V_s(\vec{r})$ is well approximated by[1]

$$V_s(\vec{r}) = \sum_i V(\vec{r} - \vec{r}_i) , \tag{1}$$

where $V(\vec{r} - \vec{r}_i)$ is the two-body potential between a gas particle at $\vec{r}$ and a constituent particle of the solid at lattice site $\vec{r}_i$. For gas-metal systems the surface potential has been constructed taking some account of the electronic degrees of freedom within the framework of the jellium model.[2]

The surface potential $V_s(\vec{r})$ will typically develop a number of bound states into which gas particles can be trapped to form the adsorbate. If, due to the structure of the surface crystal plane, $V_s(\vec{r})$ is strongly localized on specific adsorption sites in the surface, we speak of localized physisorption. In contrast, for mobile adsorption the surface potential is treated as a function only of the distance z above the uniform surface, $V_s(\vec{r}) \equiv V_s(z)$, so that adsorbed particles can move more or less unhindered along the surface. At very low coverage where the interaction between gas particles in the adsorbate can be neglected, we can base a kinetic theory of physisorption on a master equation, i.e., a system of rate equations,[3]

$$\frac{dn_{\vec{i}}}{dt} = \sum_{\vec{j}} R_{\vec{i}\,\vec{j}} n_{\vec{j}} - \sum_{\vec{j}} R_{\vec{j}\,\vec{i}} n_{\vec{i}} \tag{2}$$

for the occupation functions $n_{\vec{i}}(t)$ where $\vec{i}$ is a set of quantum numbers characterizing a bound state or continuum state of a gas particle in the surface potential $V_s(\vec{r})$. The transition probabilities $R_{\vec{i}\,\vec{j}}$ take into account bound-state—bound-state, bound-state—continuum, and continuum—bound-state transitions. Assuming that the surface potential can, for a mobile adsorbate, be adequately represented by a Morse potential and calculating the $R_{\vec{i}\,\vec{j}}$'s in second-order perturbation theory (Fermi's golden rule) for phonon-mediated processes, isothermal desorption times have been calculated from (2) for a number of systems such as ^{4}He-LiF, ^{4}He-graphite, Xe-W, etc.[3] Also, for gas-solid systems with many surface bound states, kinetic equations of the Fokker-Planck and Kramers type have been derived and studied in great detail.[4]

All these theories of physisorption kinetics and,

to the knowledge of the authors, all microscopic kinetic theories of adsorption and desorption in the literature to date, are restricted to situations of very low (zero) coverage, although phenomenological theories have been developed since Langmuir's pioneering work[5] that account for saturation effects in the kinetics as an adsorbate approaches monolayer coverage.[6] Defining (in the submonolayer range) the coverage Θ as the fraction of a monolayer adsorbed one writes for its time rate of change

$$\frac{d\Theta}{dt}=r_a-r_d\ , \tag{3}$$

where

$$r_a=P(2\pi mk_BT)^{-1/2}n_{\max}^{-1}S(\Theta,T) \tag{4}$$

is the rate of adsorption with $S(\Theta,T)$ the sticking coefficient and $n_{\max}$ the number density of adsorbed gas particles in a monolayer. Saturation is incorporated via an ansatz $S(\Theta,T)\sim(1-\Theta)$. Also, for first-order desorption one writes

$$r_d=\Theta/t_d\ , \tag{5}$$

where t_d is the desorption time which is usually given in the Frenkel-Arrhenius parametrization

$$\begin{aligned}t_d&=t_d(T,\Theta)\\&=\nu^{-1}(T,\Theta)\exp[Q(T,\Theta)/k_BT]\ ,\end{aligned} \tag{6}$$

where $\nu=\nu(T,\Theta)$ is called the prefactor and

$$Q(T,\Theta)=k_BT^2\frac{\partial \ln P}{\partial T}\bigg|_{\Theta} \tag{7}$$

is the isosteric heat of adsorption.

Ultimately the above coverage dependence arises from the two-body interaction between gas particles in the adsorbate, resulting in several different mechanisms which we want to discuss briefly. For strongly localized adsorption as it occurs in many chemisorption systems, only one particle can be adsorbed per adsorption site due to the finite size of the adsorbing particle and due to bond saturation restricting chemisorption typically to monolayer coverage. As the monolayer fills up, the long-range interaction between adsorbed particles can lead to a variety of ordered structures reflected, in particular, in characteristic changes in Q, ν, and t_d. For recent experiments see Refs. 7–9; a recent microscopic model has been analyzed by Zhdanov.[10]

Next we look at the adsorption of a gas onto a solid surface without pronounced adsorption sites. For physisorption systems this implies that the surface potential is more or less uniform along the surface, i.e., a function of the distance z above the surface only. At high temperatures gas particles in the adsorbate will then be highly mobile. With monolayer densities typically of the order of liquid densities, collisions of adparticles will probe predominantly the short-range repulsion between them, leading to a decrease in the heat of adsorption as coverage builds up. A dramatic decrease typically occurs at monolayer completion because the adparticles in the second layer are bound far more weakly to the adparticles in the first layer than the latter are to the solid. For multilayer adsorbates, Q will eventually approach the heat of vaporization of the corresponding liquid. Our theory will demonstrate these features explicitly. At lower temperature small lateral variations in the surface potential due to the lattice structure of the solid can lead to a two-dimensional commensurate crystallization in the adsorbate. In addition, the attractive part of the two-body interaction between adparticles can lead to a crystalline phase typically as an adsorbate superstructure, accompanied most likely by a rise in the heat of adsorption.

In this paper we present a mean-field theory of the kinetics of mobile multilayer physisorption. In the next section we briefly review the mean-field theory developed in two previous papers[11,12] to the extent necessary for kinetics. Section III will then contain the derivation of the nonlinear rate equations and the calculation of the phonon-mediated transition probabilities. In Sec. IV we present the calculation of desorption times for the ^{4}He-graphite, ^{3}He-graphite, ^{3}He–solid argon, and ^{3}He-Constantan systems. The most striking result is the prediction of a compensation effect in physisorption, i.e., a proportional variation in Q and $\ln\nu$ as a function of Θ. Such a compensation effect is observed quite frequently in thermally activated processes and has been established in a variety of chemisorption systems. For weakly coupled physisorbed systems we also predict a transition from first-order desorption at low coverage with a rate given by (5) to zero-order evaporation for $\Theta\gtrsim 2$ with a rate r_d independent of coverage. Section V summarizes the main points of insight.

II. MEAN-FIELD THEORY OF PHYSISORPTION

A gas particle adsorbing onto a clean surface finds itself in the bare surface potential $V_s(\vec{r})$. As the coverage builds up further, gas particles approaching the surface from the gas phase experi-

ence, in addition, the mutual forces due to the particles already adsorbed. We have, in Ref. 11, taken the latter into account in mean-field approximation by deriving from a quantum-mechanical many-body Hamiltonian spin-averaged, temperature-dependent Hartree-Fock equations

$$\left[-\frac{\hbar^2}{2m}\nabla^2_{\vec{r}_1}+V_s(\vec{r}_1)-E_{\vec{i}}\right]\psi_{\vec{i}}(\vec{r}_1)$$
$$+\sum_{\vec{j}} n_{\vec{j}}\int d\vec{r}_2 d\vec{r}_3 d\vec{r}_4 \psi^*_{\vec{j}}(\vec{r}_2)\langle \vec{r}_1,\vec{r}_2 \mid K \mid \vec{r}_3,\vec{r}_4\rangle$$
$$\times[(2s+1)\psi_{\vec{i}}(\vec{r}_3)\psi_{\vec{j}}(\vec{r}_4)$$
$$\pm\psi_{\vec{j}}(\vec{r}_3)\psi_{\vec{i}}(\vec{r}_4)]=0\,, \tag{8}$$

where $E_{\vec{i}}$ and $\psi_{\vec{i}}$ are the single-particle energies and wave functions, respectively. The upper (lower) sign holds for bosons (fermions). s is their spin and K is the effective interaction between the particles which, e.g., for fermions, can be identified as Brueckner's K matrix. The thermal occupation functions are given by

$$n_{\vec{j}}=\{\exp[\beta(E_{\vec{j}}-\mu)]\mp 1\}^{-1}\,, \tag{9}$$

where μ is the chemical potential per particle and $\beta=1/k_BT$. Because we assume that the gas phase is very large (infinite), it controls μ in equilibrium. Thus if away from the surface the gas can be described satisfactorily by the ideal gas law, then

$$\mu=k_BT\ln\frac{h^3P}{(2\pi m)^{3/2}(k_BT)^{5/2}}$$
$$=k_BT\ln(\lambda_{\rm th}^3P/k_BT)\,, \tag{10}$$

where P is the pressure in the gas phase and $\lambda_{\rm th}$ is the thermal wavelength. Virial corrections can be included in (10) if necessary.

To decouple the mean-field self-consistency in (8) from the self-consistency in calculated K, one invokes a local-density approximation. Also one observes that as long as the adsorbate remains fluid, one can assume that

$$\psi_{\vec{i}}(\vec{r})=L^{-1}\phi_i(z,\vec{q})e^{i\vec{q}\cdot\vec{\rho}}\,, \tag{11}$$

where L^2 is the surface area, $\vec{q}=(q_x,q_y)$ is a two-dimensional wave vector, $\vec{r}=(\vec{\rho},z)$, and $\vec{i}=(q_x,q_y,i)$ with i enumerating the bound states and the continuum. Inserting (11) into (8) and integrating out the lateral degrees of freedom, one obtains a set of one-dimensional integro-differential equations for $\phi_i(z,q)$ which is still too formidable to allow a numerical solution. Following Ref. 11, we replace the nonlocal K matrix by a local effective density-dependent softcore two-body interaction between He atoms within the adsorbate. This results in a highly mobile adsorbate for which $V_s(\vec{r})\equiv V_s(z)$ in our mean-field equations:

$$\left[-\frac{\hbar^2}{2m}\frac{d^2}{dz^2}+V_s(z)-\epsilon_i\right]\Phi_i(z)$$
$$+\sum_j \tilde{n}_j\int dz'\tilde{V}(z-z')\Phi_j^*(z')$$
$$\times[(2s+1)\Phi_i(z)\Phi_j(z')$$
$$\pm\Phi_i(z')\Phi_j(z)]=0\,, \tag{12}$$

with

$$\tilde{n}_j=\frac{\sigma_g^2}{L^2}\sum_{\vec{q}} n_{\vec{q}j}=(2\pi)^{-1}\sigma_g^2\int_0^\infty q\,dq\left\{\exp\left[\beta\left[\epsilon_j+\frac{\hbar^2q^2}{2m}-\mu\right]\right]\mp 1\right\}^{-1}$$
$$=\mp(2\pi)^{-1}mk_BT\sigma_g^2\hbar^{-2}\ln\{1\mp\exp[-\beta(\epsilon_j-\mu)]\} \tag{13}$$

and

$$\tilde{V}(z)=\sigma_g^{-2}\int d\vec{\rho}\,V_{\rm eff}(z,\vec{\rho})\,, \tag{14}$$

where σ_g is the range of the two-body interaction $V_{\rm eff}(\vec{r})$.

Starting from a bare Lennard-Jones interaction

$$V_2(r)=4\epsilon_g[(\sigma_g/r)^{12}-(\sigma_g/r)^6] \tag{15}$$

between isolated He atoms we have shown in Ref. 8 that (14) can be adequately parametrized by

$$\tilde{V}(z)=2\pi\epsilon_g z^{10}\{z^{10}+A\sigma_g^{10}\exp[-(z/z_1)^\alpha]\}^{-1}$$
$$\times[\tfrac{2}{5}(\sigma_g/z)^{10}-(\sigma_g/z)^4]\,, \tag{16}$$

where α is of order 10 to 15, $z_1/\sigma_g\sim 0.8$, and A is a density parameter that can be calculated for fermionic gas particles from Brueckner theory. Note that $\tilde{V}(0)=4\pi\epsilon_g/5A$ is finite. A similar effective two-body interaction has been used in a mean-field theory of ^{4}He by Bernardes and Primakoff[13] and is discussed by Brueckner and Frohberg.[14]

In Ref. 11 we have solved (12) numerically for a number of model systems to study the dependence of the single-particle energies ϵ_i, the wave functions Φ_i, the coverage, and the adlayer positions on the potential parameters in $V_s(z)$ and $\tilde{V}(z)$ and on the particle statistics. In Ref. 12 the self-consistent solutions of (12) were used to calculate the isotherms, excess specific heats, and heats of adsorption for ^{3}He and ^{4}He adsorbing on graphite.

We would like to add a few critical comments to the above version of mean-field theory. The effective two-body interaction $V_{\rm eff}$, e.g. in (14), has been constructed to account for two-body correlations. So far we have used Brueckner's K-matrix theory for fermionic particles. We are currently developing the alternative Jastrow method which is valid for both fermions and bosons. Also, the complete reduction to one dimension as used so far does not retain enough lateral interaction between the gas particles, so that for bosons our theory is only good for less than monolayer coverage. For fermions the range can be extended up to about two monolayers by introducing a momentum cutoff in (13) to ensure monolayer saturation at the right density; for details see Refs. 11 and 12.

A good intuitive tool to understand multilayer physisorption in the mean-field approximation is given by the effective, coverage-dependent surface potential

$$V_s(z,\Theta)=V_s(z)+V_{\rm mf}(z,\Theta)\ , \tag{17}$$

where $V_s(z)$ is the bare surface potential seen by a single gas particle, and $V_{\rm mf}(z,\Theta)$ is the mean-field potential generated by all other particles already adsorbed, calculated as a Slater average.[15] Examples are given in Refs. 11 and 12.

III. RATE EQUATIONS

To describe the kinetics of adsorption and desorption we must supplement the static Hamiltonian of the gas-solid system with a term accounting for energy dissipation and supply for adsorption and desorption, respectively. For weakly coupled physisorbed gas-solid systems, this arises from the coupling of the gas particles to the phonon bath of the solid.[16] We write for the total Hamiltonian

$$H=H_s+T+V_2+V_s\ , \tag{18}$$

where H_s is the phonon Hamiltonian of the solid, T is the kinetic energy of the gas particles, V_2 contains their mutual two-body interactions, and $V_s(\vec{r},t)$ is the dynamic surface potential. For a molecular solid it is given by (1) where $\vec{r}_i=\vec{r}_i(t)$ are the positions of the thermally agitated constituent particles of the solid. For mobile adsorbates with the surface potential a function of z only, one then argues that

$$\begin{aligned}V_s(\vec{r},t)&=V_s(\vec{r}-\vec{u}(t))\\&=V_s(z)-\vec{u}(t)\cdot\vec{\nabla}V_s(z)+\cdots\ ,\end{aligned} \tag{19}$$

provided one-phonon processes dominate. The displacement vector is given by

$$\vec{u}(t)=(\hbar/2\rho)^{1/2}\sum_J \omega^{-1/2}(\vec{u}^{(J)}b_J e^{-i\omega_J t}+\vec{u}^{(J)*}b_J^\dagger e^{i\omega_J t}) \tag{20}$$

in terms of phonon creation and annihilation operators $b_J^\dagger$ and b_J, respectively, of phonon mode J and energy ω_J. ρ is the mass density of the solid. The label J refers either to the proper surface modes of a semi-infinite elastic solid[17] or, in an approximate way, to bulk modes. Expanding gas-particle field operators

$$\psi(\vec{r},t)=\sum_{\vec{i}}\psi_{\vec{i}}(r)\alpha_{\vec{i}}(t) \tag{21}$$

in terms of the Hartree-Fock single-particle states, we introduce creation and annihilation operators $\alpha_{\vec{i}}^\dagger$ and $\alpha_{\vec{i}}$ for particles in these states.[18] The Hamiltonian (18) then reads

$$\begin{aligned}H=&\sum_{\vec{i}}E_{\vec{i}}\alpha_{\vec{i}}^\dagger\alpha_{\vec{i}}+\sum_J\hbar\omega_J b_J^\dagger b_J\\&+L^{-3}\sum_{\vec{i},\vec{j},J}\omega_J^{-1/2}\vec{Y}_{\vec{i}\vec{j}}\alpha_{\vec{i}}^\dagger\\&\qquad\times(b_J^\dagger e^{i\omega_J t}\vec{u}^{(J)}+b_J e^{-\omega_J t}\vec{u}^{(J)})\alpha_{\vec{j}}\\&+H_{\rm res}\ ,\end{aligned} \tag{22}$$

where

$$\vec{Y}_{\vec{i}\vec{j}}=L^3(\hbar/2\rho)^{1/2}\times\int d\vec{r}\,\psi_{\vec{i}}^*(\vec{r})\vec{\nabla}V_s(z)\psi_{\vec{j}}(\vec{r})\ . \tag{23}$$

$H_{\rm res}$ contains all other interactions of H not diagonal in the Hartree-Fock basis, in particular all terms quartic in $\alpha_{\vec{i}}^\dagger$ and $\alpha_{\vec{j}}$ and all terms with higher powers of the phonon operators. Whereas the above is accepted practice for phonon-mediated physisorption kinetics at negligible coverage, some clarifying remarks are necessary when the adsorbate reaches monolayer coverage. First, the surface loading may

change the phonon modes as has been observed in gas-solid systems with chemisorption of heavy adsorbates.[19] However, for ^{3}He and ^{4}He adsorbates we do not expect too great an effect and therefore keep the unperturbed phonon spectrum of the unloaded solid for our calculations of desorption times. Second, at monolayer coverage desorbing particles might draw the necessary energy not directly from the solid but via a collective excitation in the adsorbate itself. Such a coupling is still contained in $H_{\rm res}$ and could be incorporated explicitly in the random phase approximation. We have done a crude estimate of this way of supplying energy and found it smaller than by direct absorption of phonons. However, a careful study of the random phase approximation is under way.

To derive the rate equations (2), one solves the Heisenberg equations of motion for the particle and phonon operators in second-order perturbation theory and calculates

$$n_{\vec{i}}(t)=\mathrm{Tr}[\alpha^{\dagger}_{\vec{i}}(t)\alpha_{\vec{i}}(t)\hat{\rho}] , \tag{24}$$

where ρ is the statistical operator of a grand canonical ensemble based on the static part of the Hamiltonian (22), i.e., the Hartree-Fock and the phonon part. Taking the long-time limit (Fermi's golden rule) one eventually gets[20]

$$\frac{dn_{\vec{i}}}{dt}=\sum_{\vec{j}} R_{\vec{i}\vec{j}} n_{\vec{j}}(1\pm n_{\vec{i}}) - \sum_{\vec{j}} R_{\vec{j}\vec{i}} n_{\vec{i}}(1\pm n_{\vec{j}}) , \tag{25}$$

where for $E_{\vec{i}}<E_{\vec{j}}$,

$$R_{\vec{i}\vec{j}}=\frac{2\pi}{\hbar}\sum_J \omega_J^{-1}\,|\,\vec{Y}_{\vec{i}\vec{j}}\vec{u}_J\,|^2[n(\omega_J)+1] \times\delta(E_{\vec{i}}-E_{\vec{j}}+\hbar\omega_J) \tag{26}$$

with

$$n(\omega_J)=1/[\exp(\hbar\omega_J/k_BT)-1] \tag{27}$$

the thermal occupation function for phonons. For $E_{\vec{j}}<E_{\vec{i}}$ one has similarly

$$R_{\vec{i}\vec{j}}=\frac{2\pi}{\hbar}\sum_J \omega_J^{-1}\,|\,\vec{Y}_{\vec{i}\vec{j}}\vec{u}_J\,|^2 n(\omega_J) \times\delta(E_{\vec{j}}-E_{\vec{i}}+\hbar\omega_J) . \tag{28}$$

The plus sign in (25) holds for bosons and the minus sign for fermions.

In Ref. 20 we have looked at a model in which fermions can get trapped into a single bound state in a surface potential. In this case, (25) reads for the occupation function of this one bound state

$$\frac{dn_0}{dt}=\sum_{\vec{j}} R_{0\vec{j}} n_{\vec{j}}(1-n_0)-\sum_{\vec{j}} R_{\vec{j}0}(1-n_{\vec{j}})n_0 , \tag{29}$$

an equation which is the basis of Langmuir-type theories such as Eq. (3). Note that saturation of the single bound state is in this model not caused by the repulsion between gas particles but simply by Fermi-Dirac statistics.

In an isothermal desorption experiment, a gas-solid system is prepared in equilibrium at pressure P and temperature T. At time $t=0$ the gas pressure is reduced substantially and the time evolution of the adsorbate is measured and described by a simple rate equation $d\Theta/dt=-\Theta/t_d(\Theta)$, where $t_d(\Theta)$ is the (in general coverage-dependent) desorption time. To calculate the latter, we employ the following procedure: (1) For a gas-solid system in equilibrium at a pressure P and a temperature T, i.e., with occupation functions

$$n_{\vec{i}}=\{\exp[\beta(E_{\vec{i}}-\mu)]+1\}^{-1}$$

for a fermionic gas particle (^{3}He) where μ is the chemical potential of an ideal (classical) gas in front of the solid, the Hartree-Fock equations (12) are solved yielding single-particle wave functions $\psi_{\vec{i}}(\vec{r})=\phi_i(z)\exp(i\vec{q}\cdot\vec{\rho})$ and energies $E_{\vec{i}}=\epsilon_i+\hbar^2q^2/2m$ at a coverage $\Theta=\sum_{\vec{i}} n_{\vec{i}}/n_{\vec{i}}(\max)$, where $n_{\vec{i}}(\max)$ is the maximum occupation of the $\vec{i}$th state corresponding to monolayer density. To ensure saturation, in our theory we introduced a cutoff q_c for the summation over the two-dimensional lateral momentum $\vec{q}$ in the surface plane. (2) The transition probabilities $R_{\vec{i}\vec{j}}$ are calculated according to (26). (3) To account for the removal of the gas phase in an isothermal desorption experiment, we drop continuum-bound state transition from (25) and integrate these equations for a small increment Δt with the right-hand side determined by the initial conditions. (4) With the new occupation functions $n_{\vec{i}}(\Delta t)$ (all continuum states are empty) corresponding to a reduced coverage $\Theta(\Delta t)$, we enter the Hartree-Fock equations [step (1)] and recalculate $\psi_{\vec{i}}(\vec{r})$ and $E_{\vec{i}}$ self-consistently, after which we can return to step (2) above. In this way we generate the time evolution $\Theta(t)$ from which we can extract the time scale $t_d(\Theta)$ of

desorption. The implicit assumption in the above procedure is, of course, that the internal readjustment of the adsorbate during the desorption process is much faster than the desorption process itself. Note that in addition to the explicit nonlinearity of the rate equations (25) there is a much stronger implicit one through the dependence of the initial and final states in $R_{\vec{i}\vec{j}}$ on the $n_{\vec{i}}$'s in (26).

The above calculation can be simplified considerably after the realization that the He-graphite and similar systems remain in quasiequilibrium during the desorption process in a temperature regime where the desorption time is much larger than the time characterizing bound-state—bound-state transitions justifying the use of perturbation theory on (25) to calculate the desorption time as[4]

$$t_d^{-1}=(\pi/M_sN_s)\sum_{\vec{i}}\sum_{\vec{p}}\sum_{\vec{c}}\omega_{\vec{p}}^{-1}\left|\int d\vec{r}\,\psi_{\vec{i}}^{*}(\vec{r})\left[\frac{\partial V_s(z)}{\partial z}\right]\psi_{\vec{c}}(\vec{r})\right|^2\delta(E_{\vec{i}}-E_{\vec{c}}+\hbar\omega_{\vec{p}})n_{\vec{i}}n_{\vec{p}}^{(\mathrm{ph})}\Big/\sum_{\vec{j}}n_{\vec{j}}\,, \tag{30}$$

where $\vec{c}$ is the momentum of a gas particle in the continuum. For a graphical representation of our results we use the Frenkel-Arrhenius parametrization (6) with P the gas pressure necessary to maintain a transient coverage at a temperature T.

IV. RESULTS

A. ^{3}He on graphite

We begin our discussion of physisorption kinetics for ^{3}He atoms desorbing from the basal plane of graphite. For this system, various bare surface potentials V_s have been studied that reproduce the experimentally determined single-particle energies well.[21] Though it is known by now that there is a small lateral variation in V_s along the graphite basal plane leading to band-structure effects,[22] we cannot include them in the present one-dimensional version of our theory in which only the laterally averaged potential $V_s(z)$ enters, which we have chosen as a zeta potential,[21]

$$V_s(z)=2\pi\epsilon_s\sigma_s^6c_sa_s^{-1}d_s^{-4}\left[\tfrac{2}{5}(\sigma_s/d_s)^6\zeta(10,z/d_s)-\zeta(4,z/d_s)\right], \tag{31}$$

where

$$\zeta(n,x)=\sum_{j=0}^{\infty}(j+x)^{-n} \tag{32}$$

is a Riemann zeta function. $d_s=3.37$ Å is the distance between crystal planes and $n_s=c_s/a_s$ is the average lateral density of the basal plane whose two-dimensional unit cell of area $a_s=5.24$ Å^2 contains $c_s=2$ atoms. The underlying ^{3}He-C two-body interaction is assumed to be a Lennard-Jones 6-12 potential with parameters $\epsilon_s/k_B=16.23$ K and $\sigma_s=2.74$ Å. We have also calculated desorption times in a bare surface potential that is based on an Yukawa-6 ^{3}He-C interaction[21] and found them to be about 30% longer, a trend that follows similar conclusions on matrix elements. Because our theory is not expected to be more accurate than that, we prefer to use the bare surface potential (31) not only for ^{3}He on graphite, but also for the other systems discussed below.

The parameters ϵ_g and σ_g in the effective two-body interaction $V_{\mathrm{eff}}(z)$ in (14) are known from the underlying Lennard-Jones interaction between two isolated He atoms to be $\epsilon_g/k_B=10.22$ K and $\sigma_g=2.556$ Å. The parameters A, z_1, and α determining the soft-core repulsion are less certain. We have shown in Ref. 11 how they can be determined for a system of interacting fermions by a Brueckner-type calculation. For two ^{3}He atoms interacting in a ^{3}He fluid of liquid density, we found that $z_1\approx0.8\sigma_g$, $\alpha\approx15$, and $A\approx1.7$, which gives $\tilde{V}(0)\approx-2\tilde{V}(z=z_{\min})$, i.e., a repulsion at $z=0$ that is as high as the attraction is deep at $z=z_{\min}$. We also saw that $\tilde{V}(z=0)$ varies roughly linearly with density up to liquid density. In solving (8) self-consistently we therefore fix A at each coverage such that $\tilde{V}(0)\approx-0.2\tilde{V}(z=z_{\min})$ at $\Theta=0$ rising linearly to $V(0)\approx-2.0\tilde{V}(z=z_{\min})$ for $\Theta\geq1$. To familiarize the reader with those features of the mean-field theory of physisorption relevant to the subsequent discussion of desorption kinetics, we turn to Fig. 1. The upper panel gives the bare surface potential $V_s(z)$ in (31) at zero coverage. Indicated are the four bound-state energies; also given are the squared wave functions of the lowest two bound states. As the coverage builds up to a monolayer (center panel in Fig. 1) the effective coverage-dependent surface potential $V_s(z,\Theta)$ from (17) develops a repulsive barrier that keeps additional

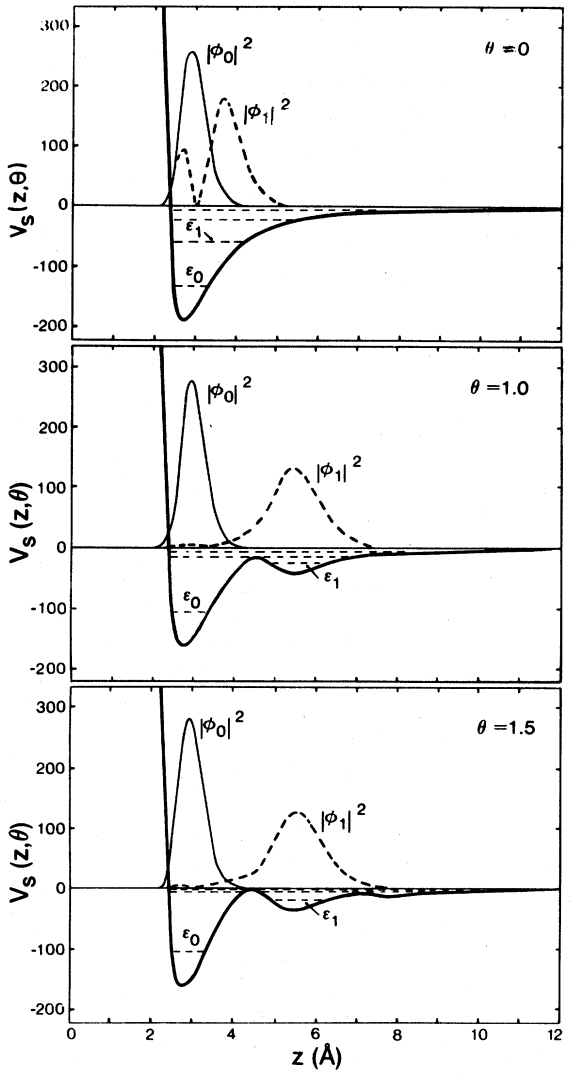

FIG. 1. Effective surface potential $V_s(z,\Theta)$ in kelvin from (17) for the ^{3}He-graphite system at $T=12$ K for three coverages; bound state energies are indicated. Also shown are squared wave functions $|\phi_0(z)|^2$ (solid line) and $|\phi_1(z)|^2$ (dashed line). Maximum monolayer coverage 0.107 Å^{-2}.

particles confined to a second adlayer. We recall that the correct saturation density in the first layer is fixed through the momentum cutoff in the occupation functions (13). Whereas the squared wave function $|\phi_0|^2$ and the energy ϵ_0 of the ground state remain more or less unchanged, the excited states get modified considerably in that their energies move up and their wave functions move out into the positions of the second ($|\phi_1(z)|^2$) and third ($|\phi_2(z)|^2$) adlayers for $\Theta>1$; see lower panel in Fig. 1. More examples of this kind and an extensive discussion have been given in Ref. 11.

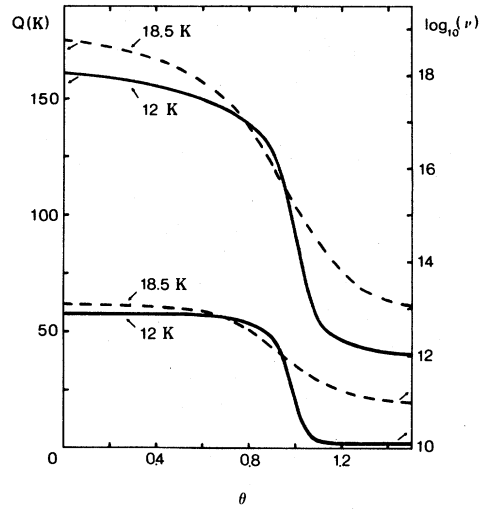

FIG. 2. Heat of adsorption Q and $\log_{10}\nu$ [see Eq. (6)] vs coverage Θ for ^{3}He-graphite at two temperatures.

In Fig. 2 we plot $\log_{10}\nu$ and Q vs Θ for $T=12$ and 18.5 K for ^{3}He desorbing from graphite. Note that Q drops from a value $Q\approx-\epsilon_0+1.5k_BT$ at $\Theta=0$, where $\epsilon_0/k_B=-135$ K is the lowest-energy state in the bare surface potential, to $Q\approx\epsilon_g+1.5k_BT$ at $\Theta\approx1.5$, where ϵ_g is the depth of the He-He interaction potential. This trend simply reflects the fact that a He atom is more tightly bound to the graphite surface than to a monolayer of heli-

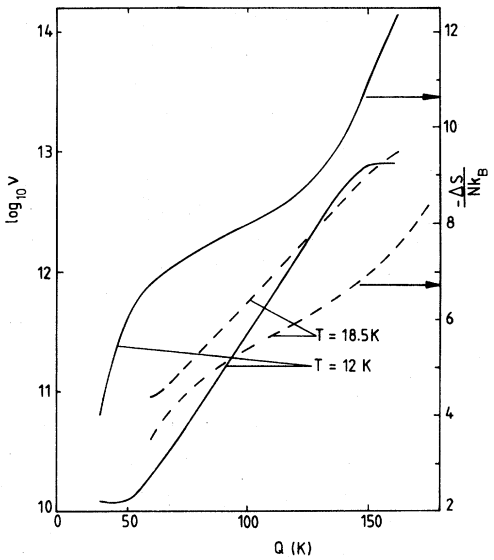

FIG. 3. $\text{Log}_{10}\nu$ and ΔS [see Eq. (34)] vs Q for ^{3}He-graphite.

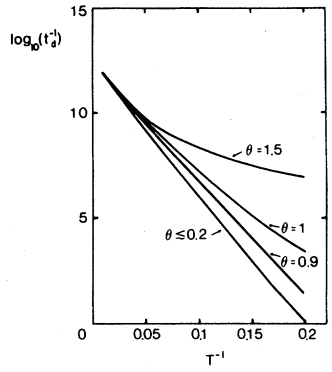

FIG. 4. $\mathrm{Log}_{10} t_d^{-1}$ vs T^{-1} for ^{3}He-graphite.

um on graphite. At the same time the prefactor drops from $\nu = 10^{13}\ \mathrm{s}^{-1}$ at $\Theta = 0$ to $\nu = 10^{10}\ \mathrm{s}^{-1}$ at $T = 12$ K and $\nu = 10^{11}\ \mathrm{s}^{-1}$ at $T = 18.5$ K for $\Theta > 1$. The rapid decrease in ν as a monolayer gets completed can be readily understood from the expression (26) for $R_{\vec{i}\vec{j}}$ and the fact that, according to the lower panel of Fig. 1, the second bound state is moving quite far out for $\Theta > 1$ into the region of the second adlayer where the coupling to the phonons, quantified by the gradient of the bare surface potential ($\vec{\nabla} V_s$) in (26), gets very weak. The fact that the prefactor ν changes in the same direction as the heat of adsorption, in particular that

$$\ln \nu = bQ + c \ , \tag{33}$$

is referred to generally for thermally activated processes as a compensation effect, and has been observed in many chemisorbed systems and "families" of similar catalysts. For an introductionary discussion we refer to Clark's book,[6] where three models are discussed as possible explanations. Indeed, Fig. 3 shows that (33) is borne out for coverages $0.1 \lesssim \Theta \lesssim 1.2$. For $\Theta \lesssim 0.1$, ν remains constant. For $\Theta \lesssim 1.5$, ν remains constant. For $\Theta \lesssim 1.5$ one expects another region of linearity between $\log_{10}\nu$ and Q. We have argued above that the compensation effect in our system has a simple microscopic explanation in the mean-field binding of an adsorbed

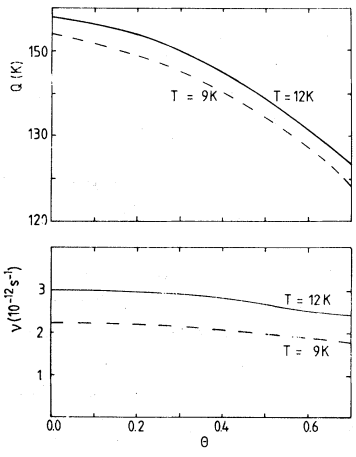

FIG. 5. Heat of adsorption Q and prefactor ν from (6) vs Θ for ^{4}He-graphite.

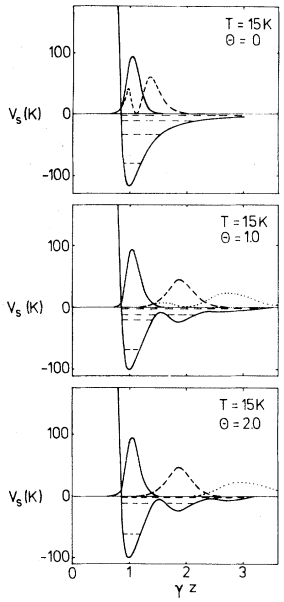

FIG. 6. Effective surface potential $V_s = V_s(z,\Theta)$ in kelvin from (17) for the ^{3}He-Ar(100) system at $T = 15$ K for three coverages; bound-state energies are indicated. Also shown are squared wave functions $|\phi_0(z)|^2$ (solid line), $|\phi_1(z)|^2$ (dashed line), and $|\phi_2(z)|^2$ (dotted line). Maximum coverage 0.08 Å^{-2}.

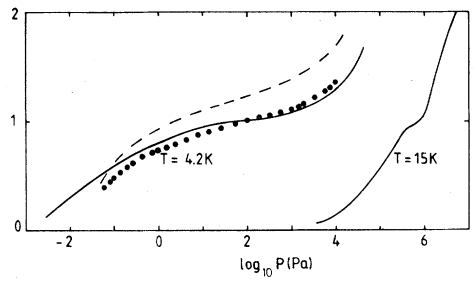

FIG. 7. Isotherms for ^{3}He-Ar(100) system. Dashed line: experimental data from Wallace and Goodstein (Ref. 28). Dotted line: "corrected" data for different maximum nonolayer coverage (see text).

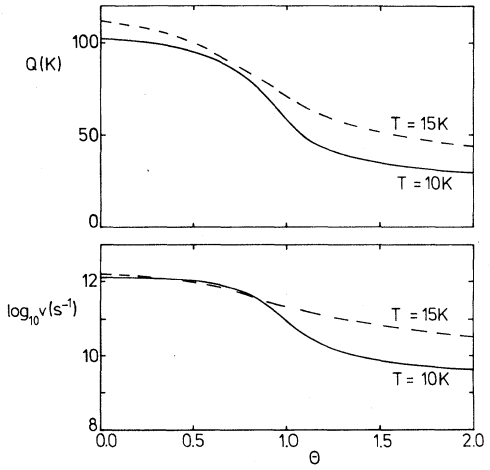

FIG. 8. Heat of adsorption Q and $\log_{10}\nu$ from (6) for ^{3}He-Ar(100).

particle, particularly around monolayer coverage, to the solid *per se* and the other adsorbed particles and in the weakening of the effective adsorbate-phonon coupling. For further corroboration, one can look for a thermodynamic explanation of the compensation effect resorting to transition rate theory which says (see, e.g., Clark's account of Kemball's model[23]) that

$$\nu \sim \exp(\Delta S/k_B) , \tag{34}$$

where $\Delta S = S_{\text{gas}} - S_{\text{ads}}$ is the entropy lost by transferring a particle from the adsorbate to the gas phase. A compensation effect is then observed if ΔS is proportional to the change of enthalpy in the above transfer, i.e., to the heat of adsorption. Indeed, this proportionality, albeit not linear, is observed in our system as seen in Fig. 3. A further illustration of the compensation effect in our system

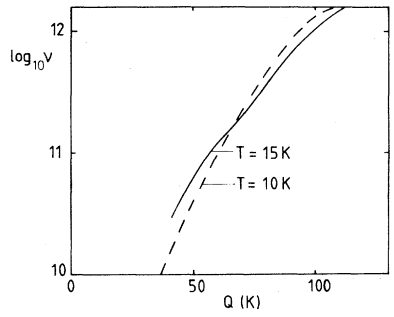

FIG. 9. $\text{Log}_{10}\nu$ vs Q for ^{3}He-Ar(100).

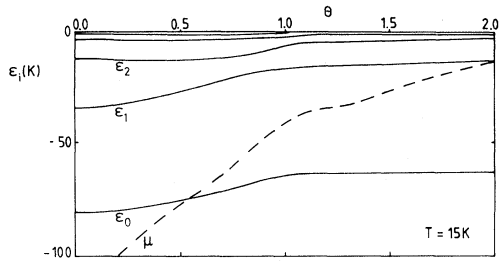

FIG. 10. Single-particle energies ϵ_i vs Θ from the mean-field equations (12) for ^{3}He-Ar(100).

can be found in Fig. 4 which shows that the curves $\log_{10}(t_d^{-1})$ vs T^{-1} for various coverages Θ indeed converge at high temperature. Because Q, the slope of $\log_{10}(t_d^{-1})$, increases more than linearly at high T, these curves do not actually cross, as textbook discussions would like to see it.

B. ^{4}He on graphite

Because the present version of our mean-field theory of physisorption does not give the correct monolayer saturation if the adsorbed particles obey Bose-Einstein statistics (see, however, the extensive discussion in Ref. 11), we calculated the desorption time for ^{4}He desorbing from the basal plane of graphite up to a coverage $\Theta \lesssim 0.7$. Figure 5 gives the heat of adsorption Q and the prefactor (not its logarithm) as a function of Q for two temperatures. The similarity to Fig. 2 for ^{3}He desorbing from graphite is striking, albeit not surprising, in view of other data, in particular thermodynamic ones, on these two systems.[12]

C. ^{3}He on solid argon

Thermodynamic data such as specific heat, isosteric heat of adsorption, and adsorption isotherms have been reported for ^{3}He and ^{4}He adsorbed on solid argon at 4.2 K.[24] We report here data for ^{3}He adsorbed on and desorbing from the (100) face of fcc argon. For the construction of the bare surface potential (13) we take the parameters of the Lennard-Jones 6-12 potential between a ^{3}He and an Ar atom to be[25] $\epsilon/k_B = 24.2$ K and $\sigma = 3.15$ Å; also $a_s = \sigma^2$ and $\sigma/d_s = 2^{1/2}$. The maximum coverage we take at $n_{\max} = 0.08$ Å^{-2}, and for solid argon we assume a Debye temperature $T_D = 92$ K. Figure 6

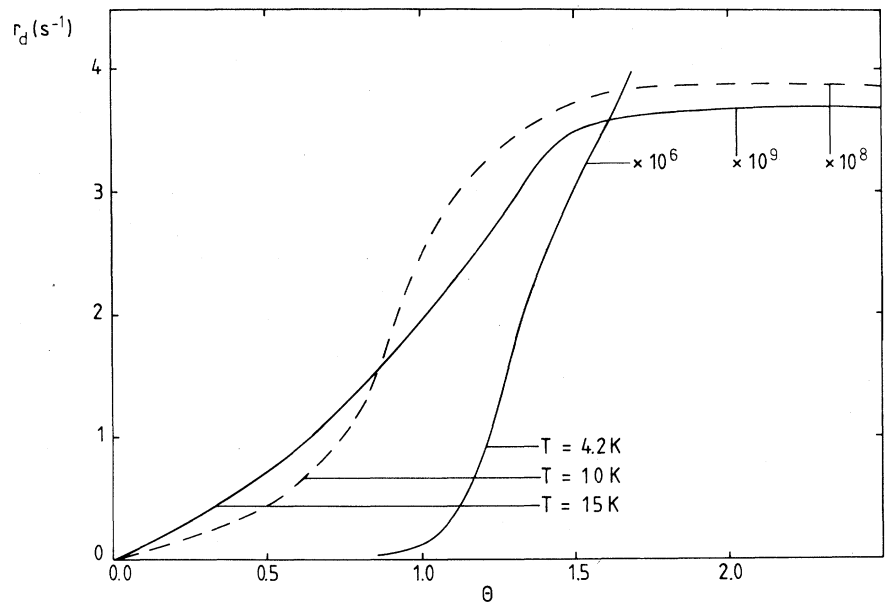

FIG. 11. Desorption rate $r_d = \Theta/t_d$ vs Θ for ^{3}He-Ar(100).

again demonstrates how the effective mean-field surface potential develops barriers and troughs to separate and accommodate second and third adlayers as Θ grows from zero to one and eventually two. To indicate the adequacy of the mean-field theory for the description of this system (^{3}He on Ar) we give in Fig. 7 two calculated isotherms together with a measured low-temperature isotherm. The discrepancy might be fortuitous for two reasons. For one, the structure of the Ar surface is not known in the experiment. Because the ^{3}He-Ar surface potential varies greatly from one surface to the other[26] a similar variation is expected for the isotherms. A second reason for the discrepancy in Fig. 7 is the fact that the monolayer coverage seems somewhat uncertain experimentally; e.g., for ^{4}He on solid argon at 4.2 K, McCormick *et al.*[24] report monolayer coverage at 15.8 cm^3 STP whereas Wallace and Goodstein[27] put it at about 20 cm^3 STP. Decreasing the experimental coverage in Fig. 7 for ^{3}He on solid argon by about the same factor 0.8, indeed, gives excellent agreement between theory and experiment (dots). In Fig. 8 we plot the heat of adsorption Q and the prefactor ν from the Arrhenius-Frenkel parametrization (6) as a function of coverage Θ for $T=10$ and 15 K. We know of no measurement of either quantity for the ^{3}He-Ar system.[28] However, Q has been measured for ^{4}He on argon[27] at $T=4.3$ K to be $Q\approx 70$ K at $\Theta=0.5$, $Q\approx 61.5$ K at $\Theta=1.0$, and $Q\approx 33$ K at $\Theta=1.5$, values that our theory also produces for ^{3}He on Ar, considering the isotopic difference. Again, $\log_{10}\nu$ varies in parallel with Q, signifying a compensation effect for this system also; see Fig. 9. It is instructive to look at the variation of the single-particle energies ϵ_i as a function of coverage Θ as depicted in Fig. 10. The fact that the energies move up as Θ increases results in the heat of adsorption Q decreasing. In addition we should observe that the energy difference $(\epsilon_1-\epsilon_0)$ increases somewhat, slowing down the desorption process as a higher-energy phonon is needed at higher Θ to accomplish desorption.

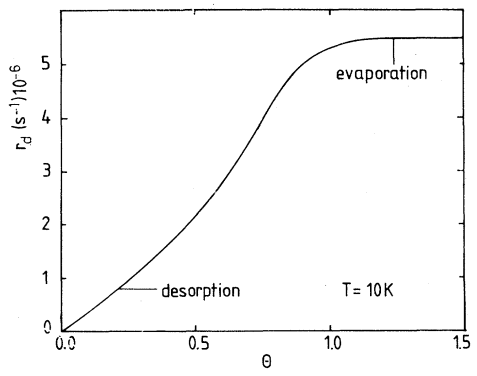

FIG. 12. Desorption rate r_d vs Θ for ^{3}He-Constantan.

With Q and ν varying so strongly as a function of

Θ, the question arises whether it is at all meaningful to write the overall desorption rate r_d as a first-order reaction according to (5). We have therefore plotted in Fig. 11 r_d vs Θ for several temperatures. At $T=10$ and 15 K it is obvious that for $\Theta \lesssim 0.5$ desorption is of first order. However, at $\Theta > 1.5$ the rate r_d becomes zero order for $T > 10$ K; i.e., desorption, proportional to coverage, goes over into evaporation at low coverage, and independent of coverage, goes over at high coverage. That evaporation sets in so early, i.e., around $\Theta \gtrsim 1.5$, we explain as arising from the rather small binding energy of ^{3}He on the substrate argon. Indeed, for ^{3}He desorbing from graphite no evaporation is predicted up to $\Theta \approx 2.0$. On the other hand, for ^{3}He desorbing from Constantan, a Cu-Ni alloy, we predict the transition from first-order desorption to zero-order evaporation at coverages slightly larger than a monolayer; see Fig. 12. For this system we have also predicted a compensation effect (^{4}He desorbing from Constantan has been measured at $\Theta \approx 1.5$ by Cohen and King[29]). A change over from first- to zero-order desorption has recently been observed in the Xe-W(110) system,[30] albeit at such quantities of adsorbed gas that uniform adsorption would be in the submonolayer regime. Our results would then suggest that the zero-order desorption of Xe from W(110) takes place from the top of multilayer patches of adsorbate, one reason being the fact that in this system the heat of adsorption also decreases only slightly upon completion of the first three adlayers.

V. CONCLUDING REMARKS

In this paper we have developed a mean-field approach to the (phonon-mediated) desorption kinetics of multilayer physisorption based on the master equation (25). To our knowledge these are the first microscopic calculations of the coverage- and temperature-dependent desorption times. Computational considerations have so far restricted us to the helium isotopes as adsorbates, the numerical examples being ^{3}He and ^{4}He on graphite, ^{3}He on Constantan (or any other metal), and ^{3}He on solid argon (or any other molecular solid). Our main results are the following: (1) The desorption rates increase with coverage, in some systems such as ^{3}He on Constantan and ^{3}He on argon changing from first-order desorption at submonolayer coverage to zero-order evaporation above a monolayer. (2) Using the Arrhenius-Frenkel parametrization (5) for the desorption time, one finds a pronounced compensation effect, i.e., a concurrent variation of Q and $\ln\nu$.

In evaluating the theory presented, a number of approximations and assumptions must be assessed both at the mean-field level and at the kinetics level. The former has been done in Refs. 11 and 12, and has been reviewed in Sec. II of this paper. Although our mean-field theory seems to be capable of reproducing most of the qualitative and some of the quantitative features of isotherms, heats of adsorption, and excess specific heat, as shown in Ref. 12 a number of improvements suggest themselves: (a) The reduction of (8) to (12) should be handled more carefully, keeping the lateral momentum dependence in $\phi_i(z,\vec{q})$ in (11) to account more fully for the saturation in the various adlayers. Indeed, a Jastrow-type approach should be tried to account for the correlations. We are working along these lines right now. (b) The lattice periodicity of the solid surface should be taken into account explicitly to allow for phase transitions in the adsorbate. This will also (c) lead to band-structure effects which so far have only been calculated by Carlos and Cole[22] at zero coverage. The energy gap in the single-particle density of states should be partially responsible for saturation.

We next turn to an assessement of the various assumptions made at the kinetic level. For weakly coupled systems, we feel not much criticism can be levied against the rate equations (2) or (25), valid quite generally for Markov processes.[31] Frequently the calculation of the transition probabilities $R_{\vec{i}\vec{j}}$, Eq. (28), as one-phonon processes is questioned. For the weakly coupled physisorbed systems studied here, we have found amble justification in Refs. 3 and 4 which draw heavily on a complete study of all two-phonon processes, also those arising from terms quadratic and cubic in $\vec{u}(t)$ in (19), which have been shown in Ref. 32 to be small for such systems. Replacing the thermal vibrations of the solid by a uniform time-dependent displacement of the surface in (19) has been rationalized in Appendix A of Ref. 3 and can be understood on the grounds that phonons of about 20% of the Debye energy, i.e., of a wavelength about 5 times a lattice constant contribute in supplying energy to the desorbing particle.

Future work on physisorption kinetics around monolayer coverage must include the possibility that the desorbing particle can, in addition to adsorbing phonons from the solid, acquire energy from collective excitations in the adsorbate, presumably very effectively below ordering transitions in

the adsorbate. They could be included in the theory via a random-phase approximation. At higher coverages of a few layers one expects intuitively that such collective excitations should become dominant.

As for generalizations of our results we venture to say that a compensation effect should be expected for phonon-mediated desorption around monolayer coverage in gas-solid systems where the phonon density of states in the surface region is not changed appreciably by the presence of the adsorbate. Local changes in surface properties (lattice or electronic) can be very pronounced in chemisorbed gas-solid systems to which the present theory is not applicable.

ACKNOWLEDGMENTS

This work was supported in part by a grant from the Natural Sciences and Engineering Council of Canada. We are indebted to Bob Teshima for writing the computer codes. This paper was written while one of us (H.J.K.) was at the Institut für Physikalische und Theoretische Chemie, University of Erlangen; thanks are due to Professor G. Wedler for his hospitality.

---

*On leave of absence from Maria-Curie-Sklodowska University, Lublin, Poland.

[1]W. A. Steele, *Interaction of Gases with Solid Surfaces* (Pergamon, Oxford, 1974).

[2]For recent contributions, see G. G. Kleiman and U. Landman, Phys. Rev. B 8, 5484 (1973); E. Zaremba and W. Kohn, *ibid.* 15, 1769 (1979).

[3]Z. W. Gortel, H. J. Kreuzer, and R. Teshima, Phys. Rev. B 22, 5655 (1980).

[4]Z. W. Gortel, H. J. Kreuzer, R. Teshima, and L. A. Turski, Phys. Rev. B 24, 4456 (1981); H. J. Kreuzer and R. Teshima, *ibid.* 24, 4470 (1981).

[5]I. Langmuir, J. Am. Chem. Soc. 40, 1361 (1918).

[6]These theories are surveyed in most books on adsorption, e.g., A. Clark, *The Theory of Adsorption and Catalysis* (Academic, New York, 1970); F. C. Tompkins, *Chemisorption of Gases on Metals* (Academic, New York, 1978); G. Wedler, *Chemisorption: An Experimental Approach* (Butterworths, London, 1976).

[7]E. Bauer, F. Bonczek, H. Poppa, and G. Todd, Surf. Sci. 53, 87 (1975).

[8]H. Pfnür, P. Fehlner, H. A. Engelhardt, and D. Menzel, Chem. Phys. Lett. 59, 481 (1978).

[9]E. Bertel and F. P. Netzer, Surf. Sci. 97, 409 (1980).

[10]V. P. Zhdanov, Surf. Sci. 111, L662 (1981).

[11]P. Summerside, E. Sommer, R. Teshima, and H. J. Kreuzer, Phys. Rev. B 25, 6235 (1982).

[12]E. Sommer and H. J. Kreuzer, Phys. Rev. B 26, 658 (1982).

[13]N. Bernardes and H. Primakoff, Phys. Rev. 119, 968 (1960).

[14]K. A. Brueckner and J. Frohberg, Suppl. Progr. Theor. Phys. 383 (1965).

[15]J. C. Slater, Phys. Rev. 81, 385 (1951).

[16]J. E. Lennard-Jones and C. Strachan, Proc. R. Soc. London Ser. A 150, 442 (1935); J. E. Lennard-Jones and A. Devonshire, *ibid.* 156, 6 (1936); 156, 29 (1936).

[17]E. Goldys, Z. W. Gortel, and H. J. Kreuzer, Surf. Sci. 116, 33 (1982); Solid State Commun. 40, 963 (1981).

[18]For technical details see, e.g., Z. W. Gortel, H. J. Kreuzer, and D. Spaner, J. Chem. Phys. 72, 234 (1980).

[19]See, e.g., H. Ibach and D. Bruchmann, Phys. Rev. Lett. 44, 36 (1980).

[20]H. J. Kreuzer and P. Summerside, Surf. Sci. 111, 102 (1981).

[21]W. E. Carlos and M. W. Cole, Surf. Sci. 91, 339 (1980). The helium-graphite interaction has been reviewed by M. W. Cole, D. R. Frankl, and D. L. Goodstein, Rev. Mod. Phys. 53, 199 (1981).

[22]W. E. Carlos and M. W. Cole, Phys. Rev. B 21, 3713 (1980).

[23]C. Kemball, Proc. R. Soc. London Ser. A 217, 376 (1953).

[24]W. D. McCormick, D. L. Goodstein, and J. G. Dash, Phys. Rev. 168, 249 (1968).

[25]For a survey of data, see *Rare Gas Solids,* edited by M. C. Klein and J. A. Venables (Academic, London, 1977).

[26]The ^{3}He-solid argon potentials have been calculated for various surfaces and found to vary greatly by M. Ross and W. A. Steele, J. Chem. Phys. 35, 862 (1961); F. Ricca, C. Pissoni, and E. Garrone, J. Chem. Phys. 51, 4079 (1969).

[27]J. L. Wallace and D. L. Goodstein, J. Low Temp. Phys. 3, 283 (1970); S. A. Cohen, Quarterly Progress Report No. 104, MIT Research Lab of Electronics (unpublished), p. 2.

[28]The data reported by T. J. Lee, Surf. Sci. 44, 389 (1974) are, in our opinion, too inconclusive to serve as a basis for a theoretical analysis.

[29]S. A. Cohen and J. G. King, Phys. Rev. Lett. 31, 703 (1973).

[30]R. Opila and R. Gomer, Surf. Sci. 112, 1 (1980).

[31]N. G. van Kampen, *Stochastic Processes in Physics and Chemistry* (North-Holland, Amsterdam, 1981).

[32]Z. W. Gortel, H. J. Kreuzer, and R. Teshima, Phys. Rev. B 22, 512 (1980).